Plasma Chem Plasma Process (2016) 36:1161–1175
DOI 10.1007/s11090-016-9704-7

ORIGINAL PAPER

Study of Condensed Phases, of Vaporization Temperatures of Aluminum Oxide and Aluminum, of Sublimation Temperature of Aluminum Nitride and Composition in an Air Aluminum Plasma

P. André[1] · M. Abbaoui[1] · A. Augeard[1,2] · P. Desprez[2] · T. Singo[2]

Received: 27 January 2016 / Accepted: 29 March 2016 / Published online: 19 April 2016

Abstract With the Gibbs free energy method, we determine the molar fraction in a plasma at and out of thermal equilibrium consisting of air and aluminum for several percentages in the temperature range of 500–6000 K. We take three temperatures into account ($T_{rot} = T_h$; T_{vib}; $T_{ex} = T_e$). We indicate the formulae and the numerical method used to perform the calculation taking three condensed phases AlN, Al, Al_2O_3 into account. We show that the air percentage plays a major role to create these phases. We clarify the role plays on the vaporization temperatures and on the sublimation temperature by the non-thermal equilibrium of the plasma. This kind of plasma is found in arc roots, near a wall, in plasmas with a high value of electrical field,… The influence of the pressures until 30×10^5 Pa. is shown on molar fraction of the chemical species, on the vaporization temperatures and on the sublimation temperature. The vaporization temperatures are given versus the thermal non equilibrium versus various mixtures (air, aluminum) and versus the pressures (10^5 Pa–30×10^5 Pa).

Keywords Aluminum nitride · Aluminum oxide · Aluminum · Plasma · Vaporization temperature · Sublimation temperature · Chemical equilibrium · Multitemperature plasma

PACS Nos. 52.27.Cm · 52.77.-j · 64.70.fm · 64.75.-g

✉ P. André
pascal.andre@univ-bpclermont.fr

[1] LAEPT, EA4646, Université Clermont Auvergne, 4 av Blaise Pascal, 63178 Aubière Cedex, France

[2] Direction de la Recherche, SAFT, 111/113, Boulevard Alfred Daney, 33074 Bordeaux Cedex, France

Introduction

In several set-ups, such as in plasma ignition technology [1], in arc tracking [2], for Current Interrupt Device (CID) inside elements of lithium-ion battery [3], for the arc welding [4] … the electrodes and the wires are made of aluminum. During the process, the interaction of air and aluminum plays a key role. Furthermore the electrical field can reach very high value that can lead the plasma to be out of thermal equilibrium (the electrons get a higher temperature than the one of heavy species). At low temperatures, the condensed phases can be conductive or insulating and then have a major influence on the electrical circuits. During the work of the set up the variation of air proportion can appear and the pressure can vary.

To model such plasmas the interaction between electrical arc and the material surface is a key parameter to improve Computational Fluid Dynamic (CFD) calculation codes [5]. To describe the arc roots, we have to know the electronic flux for example thermionic electron emission flux. This latter depends on the surface temperature of the electric contacts [6]. Thus the sublimation temperature or the vaporization temperature are fundamental to knowing when the solid sublimates or liquid vaporizes. This is used in CFD code to test when the mesh of solid or of liquid has to be replaced by a gas or plasma [7]. Furthermore, it is well known that close to the cathodic surface or close to a sheath the plasma is out of thermal equilibrium due to high electrical field or to diffusion [8]. To model these areas one has to answer to the question: are the vaporization and sublimation temperatures of the metal a function of the degree of thermal non-equilibrium?

So, the purpose of the paper is to show the influence of the air proportion, the thermal non-equilibrium and the pressures on the chemical processes, notably the condensed phases. These latter can be created after extinguishing of the electric default (electric arc, spark, hot gas…). We show that the vaporization temperatures of Al_2O_3 and Al as well as the sublimation temperature of AlN depends on the considered physical constraints.

In a first part, we depict the needed data, the physical formulae and the numerical method. In a second part, we determine the molar fraction in the temperature range of 500–6000 K versus proportion of air and aluminum at thermal equilibrium and at 10^5 Pa. In a third part, we determine molar fraction with a plasma out of thermal equilibrium. For the internal temperatures, the rotational temperature T_{rot} is assumed to be closed to the translational temperature of heavy species T_h, the excitational temperature T_{ex} closed to the translational temperature of electrons T_e and vibrational temperature T_{vib} is assumed to be intermediate between T_e and T_h as $T_{vib} = \sqrt{\theta} T_h$. The considered heavy species temperature are included between 500 K and 6000 K. The calculation are made for a mixture of 10 % of air and 90 % of aluminum, for a mixture of 50 % of air and 50 % of aluminum and for a mixture of 90 % of air and 10 % of aluminum. The vaporization temperatures and sublimation temperature are studied versus the non-thermal parameter $\theta = \frac{Te}{T_h}$. In a third part, we study the influence of pressure between 10^5 Pa until 30×10^5 Pa.

First Step Determination of Liquid Phase and Solid Phase

The dry air composition is that given by the US Standard: N_2 78.084 %; O_2 20.9476 %; Ar 0.934 %; CO_2 0.0314 % in molar percentage [9]. In the calculation we take into account the Aluminium oxide Al_2O_3 in solid phase in which we do not distinguish the various phase (α, δ, γ…), the liquid phase of Aluminium oxide, the aluminium nitride in solid

phase and the aluminum in solid and liquid phases. The liquefaction temperature of Al_2O_3 is taken equal to 2327 K [10], the liquefaction temperature of aluminum is taken equal to 933.45 K [10]. The liquid is considered to be an ideal liquid and Van der Waals interactions are neglected. The condensed phases are immiscible. We take 13 monatomic species into account: Al, Al^-, Al^+, Ar, Ar^+, C, C^-, C^+, N, N^+, O, O^-, and O^+, 23 diatomic species Al_2, AlN, AlO, AlO^-, AlO^+, C_2, C_2^-, C_2^+, CN, CN^-, CN^+, CO, CO^-, CO^+, N_2, N_2^-, N_2^+, NO, NO^-, NO^+, O_2, O_2^-, O_2^+, 31 polyatomic species Al_2O, Al_2O_2, $Al_2O_2^+$, Al_2O^+, AlO_2, AlO_2^-, C_2N, C_2N_2, C_2O, C_3, C_3O_2, C_4, C_4N_2, C_5, CNN, CNO, CO_2, CO_2^-, N_2O, N_2O_3, N_2O_4, N_2O_5, N_2O^+, N_3, NCN, NO_2, NO_2^-, NO_3, O_3, NO_3^-, CO_2^+ and electrons.

In multitemperature plasmas, following the Boltzmann distribution from populated quantum levels, one can define several kinds of temperatures: vibrational, excitational, rotational and translational. We assume that the rotational temperature, vibrational temperature, excitational temperature are the same for all the diatomic species and the excitational temperature are the same both for monatomic species and diatomic species. We assume that for all the heavy chemical species, neutral and ionic, translational temperatures have the same value. So, the translational temperatures of heavy species are the same for all kind of species omitting electrons. Usually the rotational temperature is assume to be closed to the translational temperature of heavy species and the temperature of excitational temperature closed to the translational temperature of electrons. The measurements made in several set-ups [11–13] show that the vibrational temperature is intermediate between the heavy species temperature and electronic temperature so we choose the following assumption on the temperatures:

$$\begin{cases} T_h = T_{rot} \\ T_e = T_{ex} = \theta T_h \\ T_{vib} = \sqrt{\theta} T_h \end{cases} \tag{1}$$

For all considered chemical species, the translational partition function is written as:

$$z_{tr} = \left(\frac{2\pi m_i k T_{tr}}{h^2} \right)^{3/2} \frac{k T_{tr}}{P^0} \tag{2}$$

where k is the Boltzmann constant, h the Planck constant, m_i the mass of the i chemical species, P^0 the standard pressure (10^5 Pa) and T_{tr} equal to T_e for electrons and to T_h for heavy species.

We take into account for the monatomic species, the internal partition function written as [14]:

$$z_{int} = \sum_{n,l,s} g(n,l,s) e^{-E(n,l,s)/T_{ex}} \tag{3}$$

where $g(n,l,s)$ and $E(n,l,s)$ are respectively the degeneracy and energy of the state with principal quantum number n, azimuthal quantum number l and spin s [15]. To increase the accuracy of the partition function at high temperatures, some authors [16] add levels with the help of the Ritz-Rygdberg series. Due to our temperature range between 500 and 6000 K only the low energy levels are populated [14] so we considered only the levels given in literature.

For the diatomic molecules, the treatment is the one given by Drellishak and al [17] at the thermal equilibrium. Then the internal partition function is written as:

$$z_{int} = \sum_{n=1}^{n_{max}} g_n e^{-LT_e(n)/T} \sum_{v=0}^{v_{max}(n)} e^{-LG(n,v)/T} \sum_{J=0}^{Jmax(n,v)} \frac{(2J+1)}{\sigma} e^{-LF(n,v,J)/T} \quad (4)$$

where J is the rotational quantum number; $F(n,v,J)$ is the rotational spectral term depending on the vibrational quantum v and on the electronic state n; $G(n,v)$ is the vibrational spectral term depending on the electronic state n; $T_e(n)$ the electronic spectral term of the electronic quantum state, g_n is the statistical weight of the electronic sate; σ is a

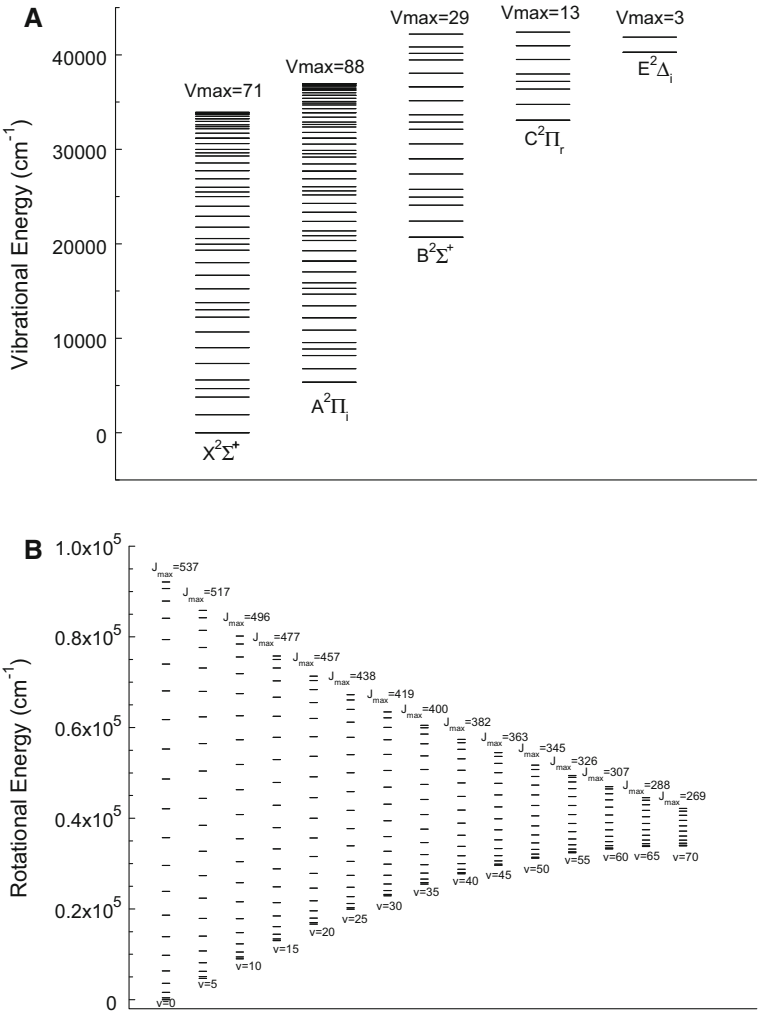

Fig. 1 **a** A representation of the vibrational levels versus electronic states taken into account for the partition function calculation of AlO. We only indicate the energies of vibration quantum multiple of 5. **b** A representation of the rotational levels versus the vibrational quantum number (multiple of 5) of the fundamental electronic state $X^2\Sigma^+$ of AlO. We only indicate the rotational energies of rotational quantum number multiple of 25

symmetry factor equal to 1 when the two atoms are different and equal to 2 when the atoms are identical.

To get the partition functions in non-thermal plasmas we separate artificially the electronic, vibrational and rotational levels as in [18] and [19]:

$$z_{int} = \left(\sum_{n=1}^{n_{max}} g_n e^{-\frac{LT_e(n)}{T_{ex}}}\right)\left(\sum_{v=0}^{v_{\max(n=1)}} e^{-\frac{LG(1,v)}{T_{vib}}}\right)\left(\sum_{J=0}^{Jmax(n=1,v=0)} \frac{(2J+1)}{\sigma} e^{-\frac{LF(1,0,J)}{T_{rot}}}\right) = Z_{ex}Z_{vib}Z_{rot} \tag{5}$$

With Z_{ex} the electronic partition function, Z_{vib} the vibrational partition function and Z_{rot} rotational partition function. That is to say, in the calculation of diatomic partition function for example AlO we only take into account the levels of the first columns of Fig. 1a, b.

The chemical potential for monatomic species is written as:

$$\mu^0_{monat} = -kT_{ex}\ln(Z_{int}) - kT_{tr}ln(Z_{tr}) + e^0 \tag{6}$$

With e_0 is the formation enthalpy of the considered chemical species.

Obviously the electronic excitation temperature and translational temperature are identical at thermal equilibrium.

The chemical species for diatomic species is written as:

- At thermal equilibrium all the temperatures are identical:

$$\mu^0_{diat} = -kT\ln(Z_{int}) - kTln(Z_{tr}) + e^0 \tag{7}$$

- And out of thermal equilibrium:

$$\mu^0_{diat} = -kT_{ex}\ln(Z_{ex}) - kT_{vib}\ln(Z_{vib}) - kT_{rot}\ln(Z_{rot}) - kT_{th}\ln(Z_{tr}) + e^0 \tag{8}$$

For the polyatomic chemical species and the condensed chemical species we take the chemical potential and the enthalpy formation in [10]. We assumed that the main constraint on the plasma properties is due to the pressure then we used the Gibbs free energy minimisation out of thermal equilibrium [20, 21]. So, the Gibbs energy of the system can be divided in three terms:

- The electrons contribution:

$$G_e = n_e\left[\mu^0_e + kT_e ln\left(\frac{T_e n_e}{T_e n_e + T_h\sum_{i=1;i\neq e}^{N_{pg}} n_i}\right) + kT_e ln\left(\frac{P}{P^0}\right)\right] \tag{9}$$

- The gaseous heavy species contribution:

$$G_{pg\_i} = \sum_{i=1}^{N_{pg}} n_i\left[\mu^0_i + kT_h ln\left(\frac{T_h n_i}{T_e n_e + T_h\sum_{i=1;i\neq e}^{N_{pg}} n_i}\right) + kT_h ln\left(\frac{P}{P^0}\right)\right] \tag{10}$$

- The liquid and solid species contribution:

$$G_{ls} = \sum_{i=1}^{N_{ls}} n_i\mu^0_i \tag{11}$$

Several numerical methods have been developed in the case of complex chemical equilibrium compositions [22], we have to modify the numerical method given in [23] and [24] to take into account all the condensed phases and the non-thermal equilibrium.

Influence of the Air Proportion

To depict the influence of air on the formation of condensed phases, we have chosen several proportions of air with pure aluminum. In Table 1, we give the vaporization temperatures (Al_2O_3, Al) and sublimation temperatures (AlN) of nine mixtures and in Fig. 2 we have plotted the molar fractions for five featured and interesting mixtures.

In Fig. 2a, we have plotted the molar fraction of chemical species versus temperature for a mixture of pure aluminum at 90 % and in dry standard air at 10 % in molar percentage at 10^5 Pa. The main condensed chemical species is the aluminum in solid phase below 933 K and in liquid phase between this latter temperature and 2767 K. The second main condensed phase is the aluminum nitride that sublimate around 2682 K. The third main condensed phase is the aluminum oxide that is in solid phase below 2327 K and liquid until its vaporization around 2387 K. The argon is an inert gas. It does not react with other chemical species. The argon is the main gaseous chemical species at the lower temperature. After the Al_2O_3 vaporization and before the AlN sublimation, the main gaseous species is the gaseous aluminum oxide (Al_2O). Then the Nitrogen is the main gaseous chemical species until the vaporization of aluminum. For the higher temperature gaseous aluminum is the main chemical gaseous species. Indeed, the ionization energy of Al_2O is 8.2 eV is lower than the ionization energy of the main gaseous molecule N_2 (15.58 eV) and it is higher than the dissociation energy of Al_2 (2.73 eV). To compare the Al_2O^+ and Al^+ ions, we have to compare their enthalpy of formation respectively (6.7 and 9.37 eV). So the Al_2O^+ ion is formed at a lower temperature than the Al^+ ion. The ionization energy of Al is 5.99 eV which is lower than the ionization energy of the other monatomic species (Ar 15.76 eV, C 11.26 eV, O 13.62 eV, N 14.53 eV). Thus, the electrical neutrality is made between electrons and Al_2O^+ until around 5000 K then the electrical neutrality is made with the aluminum ions Al^+. The main chemical reactions occur at around 4200 K. They are: the dissociation of Al_2O in AlO and Al_2 with an energy

Table 1 Vaporization temperature and sublimation temperature versus the Al and Air in molar percentage at 10^5 Pa and thermal equilibrium at thermal equilibrium ($\theta = 1$)

	T_{vap} Al (±3 K)	T_{sub} AlN (±3 K)	T_{vap} Al_2O_3 (±3 K)
10 % Air 90 % Al	2767.5	2682.5	2387.5
20 % Air 80 % Al	2727.5	2687.5	2387.5
30 % Air 70 % Al	2387.5	2682.5	2502.5
40 % Air 60 % Al	–	2657.5	2532.5
50 % Air 50 % Al	–	2572.5	2522.5
60 % Air 40 % Al	–	2502.5	3712.5
70 % Air 30 % Al	–	2457.5	3757.5
80 % Air 20 % Al	–	–	3757.5
90 % Air 10 % Al	–	–	3707.5

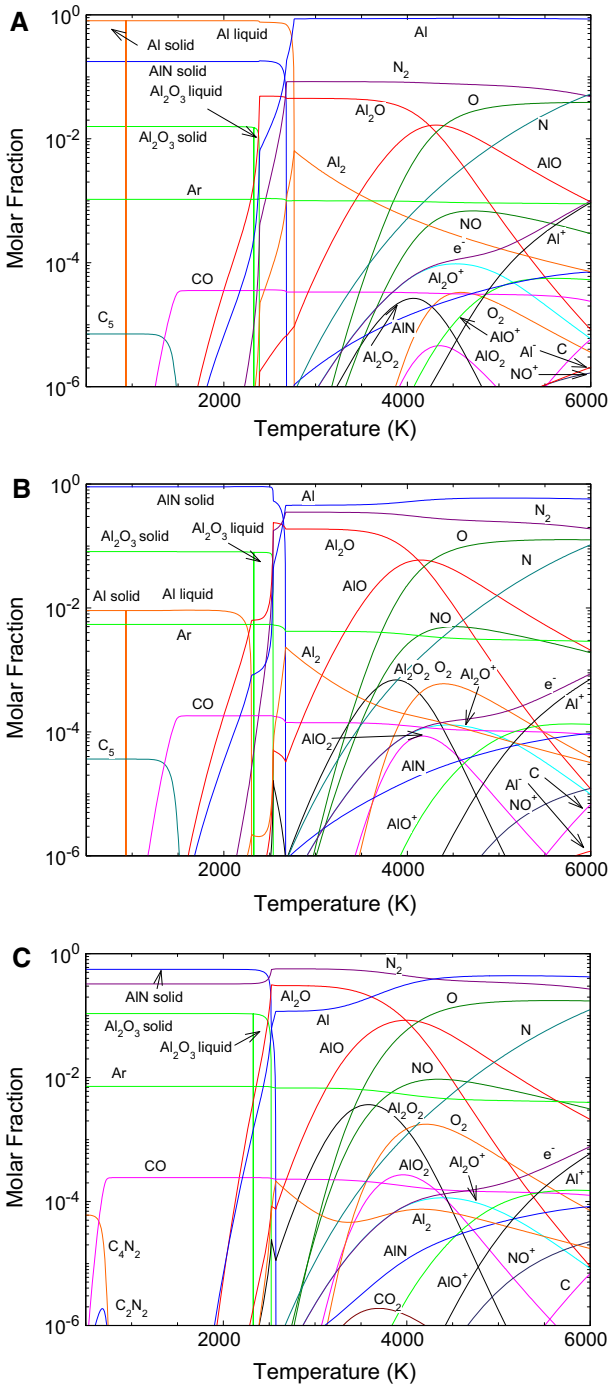

Fig. 2 **a** Molar fraction versus temperature of a mixture of 90 % aluminum and 10 % of dry standard air (in molar percentage) at 10^5 Pa and at thermal equilibrium ($\theta = 1$). **b** Molar fraction versus temperature of a mixture of 65 % aluminum and 35 % of dry standard air (in molar percentage) at 10^5 Pa and at thermal equilibrium ($\theta = 1$). **c** Molar fraction versus temperature of a mixture of 50 % aluminum and 50 % of dry standard air (in molar percentage) at 10^5 Pa and at thermal equilibrium ($\theta = 1$). **d** Molar fraction versus temperature of a mixture of 25 % aluminum and 75 % of dry standard air (in molar percentage) at 10^5 Pa and at thermal equilibrium ($\theta = 1$). **e** Molar fraction versus temperature of a mixture of 10 % aluminum and 90 % of dry standard air (in molar percentage) at 10^5 Pa and at thermal equilibrium ($\theta = 1$)

Fig. 2 continued

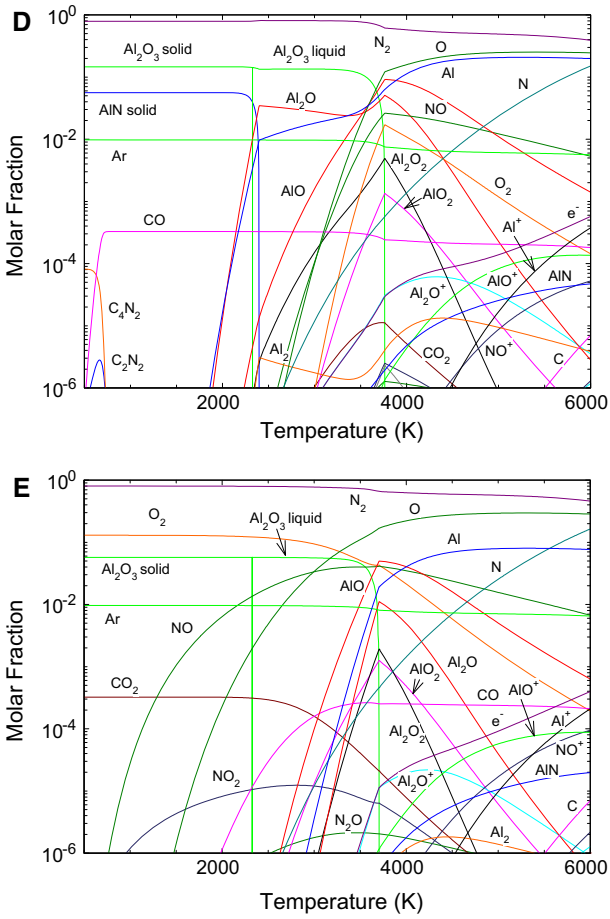

of 4.7 eV followed by the dissociation of Al_2O in AlO and Al with an energy of 5.58 eV in parallel with the dissociation of AlO in Al and O with an energy of 5.25 eV.

In Fig. 2b we have plotted the molar fraction of chemical species versus temperature for a mixture of pure aluminum at 65 % and of dry standard air at 35 % in molar percentage. The main condensed chemical species is the aluminum nitride aluminum that sublimates around 2672 K. The second main condensed phase is aluminum oxide that is in solid phase below 2327 K and liquid until its vaporization around 2537 K. The third is the aluminum in solid phase below 933 K and in liquid between this latter temperature and 2300 K. Since the initial concentration of atomic N is higher accordingly the AlN concentration is higher. An increase in the initial quantity of oxygen also increases the concentration of Al_2O_3. The argon is the main chemical species at the lower temperature. The main gaseous species are Al, N_2 and Al_2O after the Al_2O_3 vaporization. For the higher temperature gaseous aluminum is the main species. The electrical neutrality is made between electrons and Al_2O^+ until around 4500 K, between electrons with Al_2O^+, Al^+, AlO^+ between 4500 K and 5300 K and between electrons with Al^+ for higher temperature. We can notice that the

concentration of AlO^+ increases when the air percentage increases. The main chemical reaction is made around 4200 K with the dissociation of Al_2O.

In Fig. 2c we have plotted the molar fraction of chemical species versus temperature for a mixture of pure aluminum of 50 % and in dry standard air of 50 % in molar percentage. The main result is that we obtain only two main condensed chemical species. They are condensed aluminum oxide that is in solid phase below 2327 K and liquid until its vaporization around 2522 K and the aluminum nitride that sublimates around 2572 K. In fact, the number of atoms of O and N in the initial mixture is sufficient to react with condensed Al. The main gaseous chemical is Ar until 2350 K and when the Al_2O_3 vaporization occurs Al, N_2 and Al_2O. Nitrogen is the main chemical species until 4270 K and for the higher temperature gaseous aluminum is the main species. The electrical neutrality is made between electrons and Al_2O^+ until around 4500 K, between electrons with Al_2O^+, Al^+, AlO^+ between 4930 K and 5450 K and between electrons with Al^+ for higher temperature. The main chemical reaction is made around 4200 K with the dissociation of Al_2O.

In Fig. 2d, we have plotted the molar fraction of chemical species versus temperature for a mixture of pure aluminum of 25 % and in dry standard air of 75 % in molar percentage. Unlike previously, the main condensed phase is Al_2O_3 and not the aluminum nitrate. Indeed, the number of initial atom O is sufficient to react with condensed Al and AlN to produce condensed Al_2O_3. So, they are two condensed phase aluminum oxide and the aluminum nitride. The condensed phase aluminum oxide is in solid phase below 2327 K and liquid until its vaporization around 3763 K. The aluminum nitride sublimates around 2390 K. The main chemical species is nitrogen N_2 in all the considered temperature. The main gaseous chemical reaction is the dissociation of NO around 4850 K. The electrical neutrality is made between electrons and Al_2O^+ until around 4695 K, between electrons with AlO^+ between 4695 K and 5580 K and between electrons with Al^+ for higher temperature.

In Fig. 2e, we have plotted the molar fraction of chemical species versus temperature for a mixture of pure aluminum of 10 % and in dry standard air of 90 % in molar percentage. Unlike previously, we observe only one condensed phase. It is the aluminum oxide Al_2O_3. Indeed, the number of initial atom O is sufficient to react with condensed Al and AlN to produce only condensed Al_2O_3. That is in solid phase below 2327 K and liquid until its vaporization around 3700 K. The main chemical species is nitrogen N_2 in all the considered temperature. Unlike previously we do not observe at low temperature carbon oxide CO but carbon dioxide CO_2. As a matter of fact the number of O is sufficient to react with CO to produce CO_2. The main gaseous chemical reaction is the dissociation of NO around 4190 K. The electrical neutrality is made between electrons and Al_2O^+ until around 4440 K, between electrons with AlO^+ between 4440 K and 5640 K and between electrons with Al^+ for higher temperature.

Overall, it is apparent that when the proportion of air increases, the amount of the condensed chemical species Al_2O_3 and AlN increases. When there is enough oxygen in the mixture, the only condensed species is Al_2O_3, and N_2 remains in the gaseous state. Also, when the air proportion is not sufficient in the mixture, the CO molecule appears; this becomes CO_2 when the amount of oxygen is sufficient. With a low percentage of air and accordingly of O_2, the AlO^+ concentration is rather low. When the initial air concentration increases, AlO^+ become the main contributor to electrical neutrality. When the concentration of air is low, the main chemical reactions in the gaseous phase are the dissociation of Al_2O and the dissociation of AlO. In contrast, when the concentration of air is high

enough, the Al_2O_3 liquid vaporization temperature reaches a higher temperature. The main reaction is no longer the dissociation of Al_2O dissociation but the vaporization of Al_2O_3.

The Table 1 gives the vaporization temperatures and sublimation temperatures versus the molar percentage in aluminum and air. We observe that the aluminum vaporization temperature and the aluminum nitride sublimation temperature decreases when the percentage of air increases. Unlike the aluminum oxide vaporization temperature increases when the percentage of air increases.

Influence of Thermal Nonequilibrium

In Table 2, we give the vaporization temperatures and sublimation temperature (heavy species temperature) versus the Al and Air proportion in molar percentage and versus thermal non-equilibrium parameter $\theta = \frac{T_e}{T_h}$ at 10^5 Pa. In Fig. 3a, b we have plotted the molar fraction versus temperature of a mixture of 90 % aluminum and 10 % of dry standard air (in molar percentage) and a mixture of 10 % aluminum and 90 % of dry standard air at 10^5 Pa and for thermal non equilibrium parameter $\theta = 2$.

For the mixture of 90 % aluminum and 10 % of dry standard air, we observe that the solid phase of aluminum is mainly in chemical equilibria with monatomic species Al; the aluminum nitride is in chemical equilibria with Al and nitrogen N_2, the condensed phase of the aluminum oxide Al_2O_3 is in chemical equilibria with Al_2O and Al. The Al_2O is in chemical equilibria with AlO and O. Comparing the Figs. 2a and 3a, we observe that the electronic concentration increases with parameter θ for a given heavy species temperature. So the ionization of AlO appears at lower heavy species temperature. One other characteristic for ionized chemical species is that at thermal equilibrium (Fig. 2a) the main ionized chemical species is Al_2O^+ for temperatures lower than around 5000 K and Al^+ for higher temperature in the considered temperature range. Unlike in the plasma out of thermal equilibrium (Fig. 3a) the main ionic chemical species that follow one to another are Al_2O^+ until 3850 K, AlO^+ until 4725 K, succeed Al^+ in our heavy species temperature range.

For the mixture of 10 % aluminum and 90 % of dry standard air, we observe, the condensed phase of the aluminum oxide Al_2O_3 is in chemical equilibria with AlO, and Al and O. Comparing Figs. 2e and 3b, the ionization of AlO and Al_2O appear at lower heavy

Table 2 Vaporization temperature and sublimation temperature (heavy species temperature) versus the Al and Air in molar percentage and versus thermal non-equilibrium parameter $\theta = T_e/T_h$.at 10^5 Pa

	10 % Air 90 % Al			50 % Air 50 % Al			90 % Air 10 % Al		
	T_{vap} Al (±3 K)	T_{sub} AlN (±3 K)	T_{vap} Al_2O_3 (±3 K)	T_{vap} Al (±3 K)	T_{sub} AlN (±3 K)	T_{vap} Al_2O_3 (±3 K)	T_{vap} Al (±3 K)	T_{sub} AlN (±3 K)	T_{vap} Al_2O_3 (±3 K)
$\theta = 1$	2767.5	2682.5	2387.5	–	2572.5	2522.5	–	–	3707.5
$\theta = 1.5$	2587.5	2577.5	2360.0	–	2497.5	3457.5	–	–	3530.0
$\theta = 2$	2437.5	2487.5	2322.5	–	2462.5	3325.0	–	–	3347.5
$\theta = 2.5$	2297.5	2407.5	2252.5	–	2412.5	3150.0	–	–	3155.0
$\theta = 3$	2172.5	2330.0	2162.5	–	2342.5	2932.5	–	–	2935.0

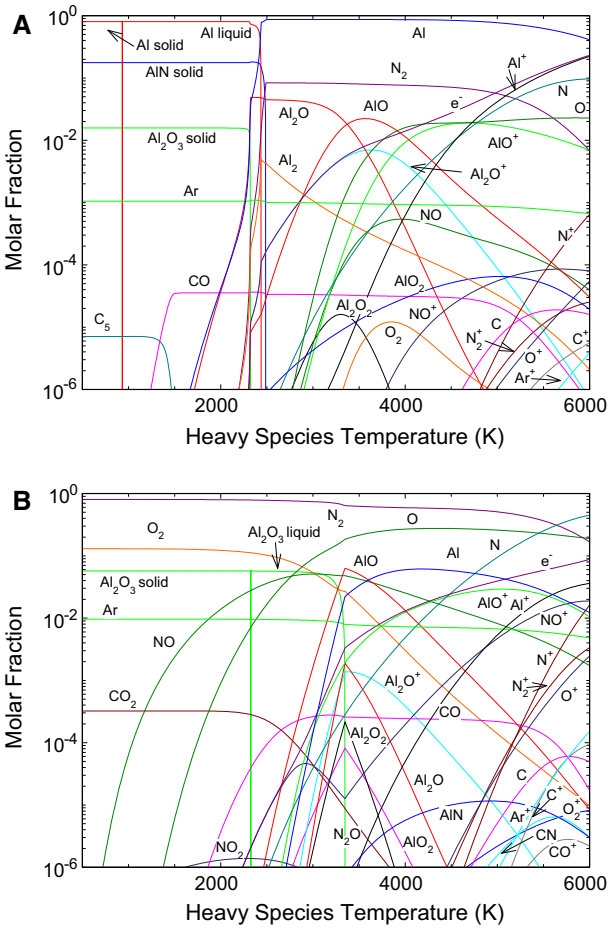

Fig. 3 **a** Molar fraction versus temperature of a mixture of 90 % aluminum and 10 % of dry standard air (in molar percentage) at 10^5 Pa and for thermal non equilibrium parameter $\theta = 2$. **b** Molar fraction versus temperature of a mixture of 10 % aluminum and 90 % of dry standard air (in molar percentage) at 10^5 Pa and for thermal non equilibrium parameter $\theta = 2$

species temperature. One other characteristic for ionized chemical species is that at out of thermal equilibrium the main ionized chemical species is AlO^+ for temperatures lower than around 5550 K and Al^+ for higher temperature in the considered temperature range. Unlike in the plasma at thermal equilibrium, the ionized chemical species follow one to another successively Al_2O^+ until 4400 K AlO^+ until 5650 K and Al^+ in our heavy species temperature range.

The energy inside the plasma is higher for a given heavy species temperature. The electronic molar fraction increases and the dissociation temperature decreases when the thermal non-equilibrium increases. The vaporization temperature and sublimation temperature (heavy species temperature) follow the same trend. As a matter of fact, the excitation temperature for monatomic species and diatomic species is assumed to be close to electronic temperature. The chemical equilibrium is made between gaseous chemical species and condensed phases. We can notice the following featured atoms and molecules: Al gaseous with Al liquid and N_2 and Al with AlN solid and AlO with Al_2O_3 liquid. The thermal equilibrium state can be estimated from an energy balance [25]. Then from the fitting coefficients of Table 3 one can evaluate the vaporization temperatures and the

Table 3 Fitting coefficients of temperatures versus thermal nonequilibrium parameter (* with $T = a\theta^2 + b\theta + c$; ** with $T = a\theta^3 + b\theta^2 + c\theta + d$)

	10 % Air 90 % Al			50 % Air 50 % Al			90 % Air 10 % Al
	T_{vap} Al*	T_{sub}AlN *	$T_{vap}Al_2O_3$*	T_{sub} AlN**	T_{vap} Al_2O_3* $\theta < 1.4$	T_{vap} Al_2O_3* $\theta \geq 1.4$	T_{vap} Al_2O_3*
a	34.3	18.6	−45.0	−40	−62.5	−90.8	−27.1
b	−433	−249	68.5	239	86.3	61.2	−275
c	31.65	2912	2363	−549	2499	3566	4008
d				2923			

sublimation temperatures that can be used in a CFD code or for resolution of the Stefan problem [26].

Influence of the Pressure

In Table 4, we give the vaporization temperatures and sublimation temperature versus the Al and air proportion in molar percentage and versus the pressure (10^5–30×10^5 Pa) at thermal equilibrium ($\theta = 1$). In Fig. 4a, b, we have plotted molar fractions versus temperature of a mixture of 90 % aluminum and 10 % of dry standard air and of 10 % aluminum and 90 % of dry standard air (in molar percentage) at thermal equilibrium and for a pressure of 15×10^5 Pa.

About the presence of condensed phase the same conclusion can be made than at 10^5 Pa (§II). For the mixture of 90 % aluminum and 10 % of dry standard air, comparing Figs. 4a and 2a, we observe that the vaporization temperatures and sublimation temperature are higher for higher pressures. The dissociation of Al_2O appearing about 4250 K at 10^5 Pa appears around 5100 K for a pressure of 15×10^5 Pa. The same behavior can be observed for the ionization the neutrality between electrons and Al_2O^+ is made for higher temperature.

For the mixture of 10 % aluminum and 90 % of dry standard air, comparing Figs. 2e and 4b, we observed that the vaporization temperature of the aluminum oxide increases.

Table 4 Vaporization temperature and sublimation temperature versus the Al and Air in molar percentage and versus pressures at thermal equilibrium ($\theta = 1$)

	10 % Air 90 % Al			50 % Air 50 % Al			90 % Air 10 % Al		
	T_{vap} Al (±3 K)	T_{sub} AlN (±3 K)	T_{vap} Al_2O_3 (±3 K)	T_{vap} Al (±3 K)	T_{sub} AlN (±3 K)	T_{vap} Al_2O_3 (±3 K)	T_{vap} Al (±3 K)	T_{sub} AlN (±3 K)	T_{vap} Al_2O_3 (±3 K)
P = 1 10^5 Pa	2767.5	2682.5	2387.5	–	2572.5	2522.5	–	–	3707.5
P = 5 10^5 Pa	3162.5	2895.0	2665.0	–	2800.0	2735.0	–	–	4040.0
P = 10 10^5 Pa	3372.5	2985.0	2805.0	–	2915.0	2840.0	–	–	4205.0
P = 15 10^5 Pa	3512.5	3037.5	2885.0	–	2985.0	2905.0	–	–	4310.0
P = 20 10^5 Pa	3617.5	3075.0	2945.0	–	3040.0	2952.5	–	–	4387.5
P = 25 10^5 Pa	3702.5	3105.0	2992.5	–	3080.0	2992.5	–	–	4450.0
P = 30 10^5 Pa	3777.5	3130.0	3030.0	–	3115.0	3022.5	–	–	4500.0

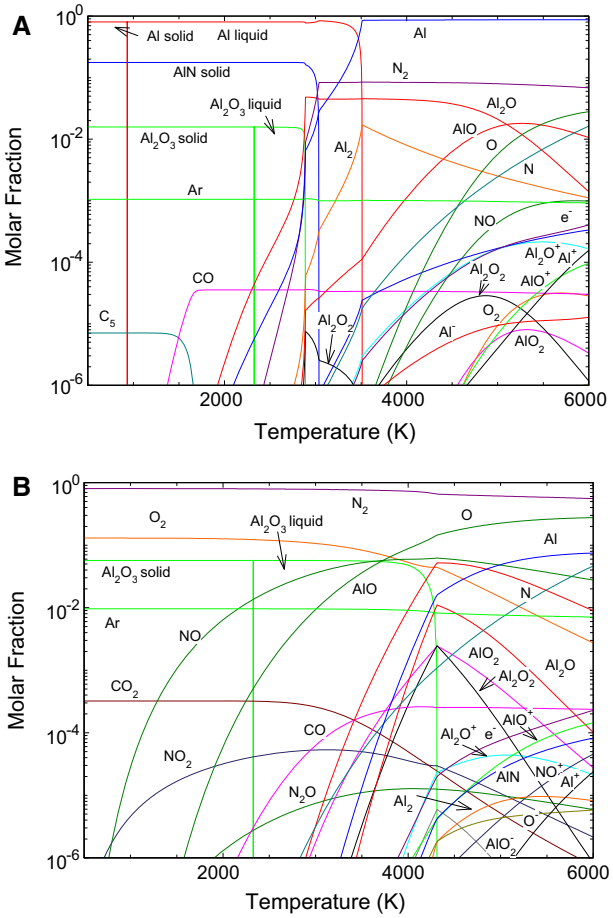

Fig. 4 **a** Molar fraction versus temperature of a mixture of 90 % aluminum and 10 % of dry standard air (in molar percentage) at thermal equilibrium ($\theta = 1$) and for a pressure of 15 bars. **b** Molar fraction versus temperature of a mixture of 10 % aluminum and 90 % of dry standard air (in molar percentage) at thermal equilibrium ($\theta = 1$).and for a pressure of 15 bars

The dissociation temperature increases consequently the electrical neutrality is made between electrons and AlO^+ for higher temperatures. When the pressure increases, the vaporization temperature increases and the condensed phase can appear at higher temperatures. Indeed, Le Chatelier's principle demonstrates that an increase in system pressure causes the chemical reactions to shift to the side with the fewer moles of gas [27]. So for example the reaction: $Al_2O \rightarrow AlO + Al$ is shifted to higher temperatures when the pressure increases.

Conclusion

The molar fraction in a plasma at and out of thermal equilibrium, with three temperatures taken into account ($T_{rot} = T_h; T_{vib} = \sqrt{\theta} T_h; T_{ex} = T_e = \theta T_h$), consisting of air and

aluminum for several percentages in the temperature range of 500–6000 K have been calculated with the Gibbs free energy method. The condensed phases of AlN (sol), Al (liq,sol) and Al_2O_3 (liq,sol) have been taken into account. Then the vaporization temperatures of Al_2O_3 and Al and the sublimation temperature of AlN have been calculated with an accuracy of ± 3 K.

We have shown that the air percentage plays a major role to create these condensed phases: at high proportion of air we get one condensed chemical species (Al_2O_3) unlike at the low proportion of air where we get three condensed phases (Al, AlN, Al_2O_3). Concerning the pressure and the thermal non equilibrium, they play the major role on the value of the vaporization temperatures and on the sublimation temperature. The values of these considered temperatures increases when the pressure increases. We have clarified the role play on the vaporization temperatures and the sublimation temperature by the non-thermal equilibrium. We have shown that the variation in the vaporization and sublimation temperatures can reach 800 K. This leads to large changes in the ablation processes that occur, for example in the cathodic arc root [6]. We have discussed the gaseous chemical species in chemical equilibrium with the condensed phase. Theoretical results can explain several behavior of set up when the condensed phase is created notably by electrical conductivity that are different one to another condensed phases [28] appearing after extinguishing of the electric arc or the plasma. The chemical species leading to the electrical neutrality have been studied during the plasma phase. One featuring chemical species is the diatomic AlO that can be used to evaluate the temperatures inside the plasma and of which concentration depends on the pressure and air proportion. Notably, the chemical equilibria between Al_2O_3(sol) and AlO Al and O. We can notice that the presence of CO_2 in standard air can be neglected since the purity of aluminum and the humidity cannot reach such level of purity. The real mixture is contaminated by pollutants originating from the aluminum. We have shown that for a given mixture of air and aluminum the same condensed chemical species appearing at 10^5 Pa. appear at higher pressures at higher temperatures.

References

1. André P (1995) Partition functions and concentrations in plasmas out of thermal equilibrium. IEEE Trans Plasma Sci 23(3):453
2. André P, Koalaga Z (2010) Composition of a thermal plasma formed from PTFE with copper in non-oxidant atmosphere Part I Definition of a test case with the SF6. High Temp Mater Process Int Q High-Technol Plasma Process 14(3):285–294
3. André P, Lefort A (1998) The influence of thermal disequilibrium on a plasma consisting of insulator vapours. J Phys D Appl Phys 31(6):717
4. André P, Barinov Y, Faure G, Shkol'nik S (2011) Modelling radiation spectrum of a discharge with two liquid non-metallic (tap-water) electrodes in air at atmospheric pressure. J Phys D Appl Phys 44(37):375203
5. André P, Bussière W, Coulbois A, Gelet J, Rochette D (2016) Modelling of electrical conductivity of a silver plasma at low temperature. Plasma Sci Technol (accepted)
6. Aubreton J, Elchinger M, André P (2013) Influence of Partition Function and Intercation Potential on Transport Properties of Thermal Plasmas. Plasma Chem Plasma Process 33(1):367–399
7. Augeard A, Desprez P, Singo T, Abbaoui M (2015) Observation par caméra rapide des spots cathodiques dans l'air au niveau du CID des éléments batterie lithium-ion. JITIPEE 1:1–9
8. Capitelli M, Molinari E (1970) Problems of determination of high temperature thermodynamic properties of rare gases with application to mixtures. J Plasma Phys 4(2):335–355
9. Chase MW (1998) NIST-JANAF thermochemical tables (Journal of physical and chemical reference data monograph No. 9), 4th edn. American Chemical Society and the American Institute of Physics for NIST (National Institute of Standards and Technology)

10. Drellishak K, Aeschliman D, Cambel Ali Bulent (1965) Partition functions and thermodynamic properties of nitrogen and oxygen plasmas. Phys Fluids 8(9):1590
11. Dricot F, Reher H (1994) Survey of arc tracking on aerospace cables and wires. IEEE Trans Dielectr Electr Insul 1(5):896–903
12. Fridman A, Kennedy L (2004) Plasma physics and engineering. Taylor & Francis, New York
13. Giordano D, Capitelli M (2002) Nonuniqueness of the two temperature Saha equation and related consideration. Phys Rev E 65:016401
14. Giordano D, Capitelli M (1995) Two-temperature Saha Equation a misunderstood problem. J Thermophys Heat Transfer 9(4):803
15. Gordon S, McBride B (1976) Computer Program for calculation of complex chemical equilibrium compositions, Rocket Performance Incident and reflected shocks and chapman jouguet detonation. NASA
16. Haynes W, Lide D, Bruno T (2012) CRC Handbook of chemistry and physics, 93rd edn. CRC Press, Taylor & Francis Group
17. Lefort A, Abbaoui M (2012) Theory about arc root: a review. IOP Cof Ser Mater Sci Eng 29:012006
18. Lesaint P, Touzani R (1989) Approximation of the heat equation in a variable doamin with application to the Stefan problem. SIAM J Numer Anal 26(2):366–379
19. Murphy AB (2015) Why the arc and its interactions with the electrodes are important in predictive modelling of arc welding. Plasma Phys Technol 2(3):233–240
20. Murphy A, Tanaka M, Yamamoto K, Sato T, Lowke J (2009) Modelling of thermal plasmas for arc welding: the role of the shielding gas properties and of metal vapour. J Phys D Appl Phys 42:194006
21. NIST. (s.d.). Récupéré sur NIST Atomic Spectra Database Levels Data: http://physics.nist.gov/PhysRefData/ASD/levels_form.html
22. Raja LL, Varghese P, Wilson D (1997) Modeling of the electrothermal ignitor metal vapor plasma for electrothermal-chemical guns. IEEE Trans Magn 33(1):316–321
23. Rochette D, Bussière W, André P (2004) Composition, enthalpy, and vaporization temperature calculation of Ag–SiO_2 plasmas with air in the temperature range from 1000 to 6000 K and for pressure included between 1 and 50 bars. Plasma Chem Plasma Process 24(3):475–492
24. Rong M, Wang W, Yan J, Murphy A, Spencer J (2011) Thermophysical properties of nitrogen plasmas under thermal equilibrium and non-equilibrium conditions. Phys Plasmas 18:113502. doi:10.1063/1.3657426
25. Rossignol J, Abbaoui M, Clain S (2000) Numerical modelling of thermal ablation phenomena due to a cathodic spot. J Phys D Appl Phys 33:2079–2086
26. Staack D, Bakhtier F, Gutsol A, Fridman A (2005) Characterization of a dc atmospheric pressure normal glow discharge. Plasma Sour Sci Technol 14(4):700–711
27. Zhao TL, Xu Y, Song YH, Li XS, Liu JL, Liu JB, Zhu AM (2013) Determination of vibrational and rotational temperatures in a gliding arc discharge by using overlapped molecular emission spectra. J Phys D Appl Phys 46(34):345201
28. Wade K, Banister A (1975) The chemistry of aluminium, gallium, indium and thallium. Pergamon Press, Oxford